

# Signal Recovery from $\ell_p$ Pooling Representations

Joan Bruna<sup>1</sup>, Arthur Szlam<sup>2</sup>, and Yann LeCun<sup>1</sup>

<sup>1</sup>Courant Institute, New York University, New York, NY

<sup>2</sup>CUNY, New York, NY

February 16, 2019

## Abstract

In this work we compute lower Lipschitz bounds of  $\ell_p$  pooling operators for  $p = 1, 2, \infty$  as well as  $\ell_p$  pooling operators preceded by half-rectification layers. These give sufficient conditions for the design of invertible neural network layers. Numerical experiments on MNIST and image patches confirm that pooling layers can be inverted with phase recovery algorithms. Moreover, the regularity of the inverse pooling, controlled by the lower Lipschitz constant, is empirically verified with a nearest neighbor regression.

## 1 Introduction

A standard architecture for deep feedforward networks consists of a number of stacked modules, each of which consists of a linear mapping, followed by an elementwise nonlinearity, followed by a pooling operation. In this work we will explore the invertibility of these layers, using the half rectification nonlinearity and  $\ell_p$  pooling, for  $p \in \{1, 2, \infty\}$ .

### 1.1 $\ell_p$ pooling

The purpose of the pooling layer in each module is to give invariance to the system, perhaps at the expense of resolution. This is done via a summary statistic over the outputs of groups of nodes. In the trained system, the columns of the weight matrix corresponding to nodes grouped together often exhibit similar characteristics, and code for perturbations of a template [7, 6].

The summary statistic in  $\ell_p$  pooling is the  $\ell_p$  norm of the inputs into the pool. That is, if nodes  $x_{I_1}, \dots, x_{I_l}$  are in a pool, the output of the pool is

$$(|x_{I_1}|^p + \dots + |x_{I_l}|^p)^{1/p},$$

where as usual, if  $p \rightarrow \infty$ , this is

$$\max(|x_{I_i}|, \dots, |x_{I_l}|).$$

If the outputs of the nonlinearity are nonnegative (as for the half rectification function), then  $p = 1$  corresponds to average pooling, and the case  $p = \infty$  is max pooling.

## 1.2 Phase reconstruction

Given  $x \in \mathbb{R}^n$ , a classical problem in signal processing is to recover  $x$  from the absolute values of its (1 or 2 dimensional) Fourier coefficients, perhaps subject to some additional constraints on  $x$ ; this problem arises in speech generation and X-ray imaging [9]. Unfortunately, the problem is not well posed- the absolute values of the Fourier coefficients do not nearly specify  $x$ . For example, the absolute value of the Fourier transform is invariant to rotations of the coordinates. It can be shown (and we discuss this below) that the absolute value of the inner products between  $x$  and any basis of  $\mathbb{R}^n$  are not enough to uniquely specify an arbitrary  $x$ ; the situation is worse for  $\mathbb{C}^n$ . On the other hand, recent works have shown that by taking a redundant enough dictionary, the situation is different, and  $x$  can be recovered from the modulus of its inner products with the dictionary [1, 4, 11].

Suppose for a moment that there is no elementwise nonlinearity in our feedforward module, and only a linear mapping followed by a pooling. Then with a slightly generalized notion of phase, where the modulus is the  $\ell_p$  norm of the pool, and the phase is the  $\ell_p$  unit vector specifying the “direction” of the inner products in the pool, the phase recovery problem above asks if the module loses any information. The  $\ell_2$  case has been recently studied in [3]

## 1.3 What vs. Where

If the columns of the weight matrix in a pool correspond to related features, it can be reasonable to see the entire pool as a “what”. That is, the modulus of the pool indicates the relative presence of a grouping of (sub)features into a template, and the phase of the pool describes the relative arrangement of the subfeatures, describing “where” the template is, or more generally, describing the “pose” of the template.

From this viewpoint, phase reconstruction results make rigorous the notion that given enough redundant versions of “what” and throwing away the “where”, we can still recover the “where”.

## 1.4 Main Contributions

In this work we will extend the  $\ell_2$  results of [3, 2] to the  $\ell_p$  case, and take into account the half rectification nonlinearity. We thus give conditions so that a module consisting of a linear mapping, perhaps followed by a half rectification, followed by an  $\ell_p$  pooling preserves all the information in its input.

We then note that the alternating minimization method of [5] can be used essentially unchanged for the  $\ell_p$  case, with or without rectification, and show experiments giving evidence that recovery is roughly equally possible for  $\ell_1$ ,  $\ell_2$ , and  $\ell_\infty$  using this algorithm; and that half rectification before pooling can recovery easier. Furthermore, we show that with a trained initialization, the alternating method compares favorably with the recovery methods in [11, 4].

## 2 Injectivity and Lipschitz stability of Pooling Operators

This section studies necessary and sufficient conditions guaranteeing that pooling representations are invertible. It also computes upper and lower Lipschitz bounds, which are tight under certain configurations.

Let us first introduce the notation used throughout the paper. Let  $\mathcal{F} = \{f_1, \dots, f_m\}$  be a real frame of  $\mathbb{R}^n$ , with  $m > n$ . The frame  $\mathcal{F}$  is organized into  $K$  disjoint blocks  $\mathcal{F}_k = \{f_j\}_{j \in I_k}$ ,  $k = 1 \dots K$ , such that  $I_k \cap I_{k'} = \emptyset$  and  $\bigcup_k I_k = \{1 \dots m\}$ .

The  $\ell_p$  pooling operator  $P_p(x)$  is defined as the mapping

$$x \mapsto P_p(x) = \{\|\mathcal{F}_k^T x\|_p, k = 1 \dots K\} . \quad (1)$$

A related representation, which has gained popularity in recent deep learning architectures, introduces a point-wise thresholding before computing the  $\ell_p$  norm. If  $\alpha \in \mathbb{R}^m$  is a fixed threshold vector, and  $(\rho_\alpha(x))_i = \max(\alpha_i, x_i)$ , then the  $\ell_p$  *rectified pooling* operator  $R_p(x)$  is defined as

$$x \mapsto R_p(x) = \{\|\rho_{\alpha_k}(\mathcal{F}_k^T x)\|_p, k = 1 \dots K\} , \quad (2)$$

where  $\alpha_k$  contains the coordinates  $I_k$  of  $\alpha$ .

We shall measure the stability of the inverse pooling with the Euclidean distance in the representation space. Given a distance  $d(x, x')$  in the input space, the Lipschitz bounds of a given operator  $\Phi(x)$  are defined as the constants  $0 \leq A \leq B$  such that

$$\forall x, x' , \quad Ad(x, x') \leq \|\Phi(x) - \Phi(x')\|_2 \leq Bd(x, x') .$$

In the remainder of the paper, given a frame  $\mathcal{F}$ , we denote respectively by  $\lambda_-(\mathcal{F})$  and  $\lambda_+(\mathcal{F})$  its lower and upper frame bounds. If  $\mathcal{F}$  has  $m$  vectors and  $S \subset \{1m\}$ , we denote  $\mathcal{F}_S$  the frame obtained by keeping the vectors indexed in  $S$ . Finally, we denote  $S^c$  the complement of  $S$ .

### 2.1 Absolute value and Thresholding nonlinearities

In order to study the injectivity of pooling representations, we first focus on the properties of the operators defined by the point-wise nonlinearities.

The properties of the *phaseless* mapping

$$x \mapsto M(x) = \{|\langle x, f_i \rangle|, i = 1 \dots m\}, \quad x \in \mathbb{R}^n, \quad (3)$$

have been extensively studied in the literature [1, 2], in part motivated by applications to speech processing [?] or X-ray crystallography [9]. It is shown in [1] that if  $m > 2n - 1$  then it is possible to recover  $x$  from  $M(x)$ , up to a global sign change. In particular, [2] recently characterized the stability of the phaseless operator, that is summarized in the following proposition:

**Proposition 2.1 ([2], Theorem 4.3)** *Let  $\mathcal{F} = (f_1, \dots, f_m)$  with  $f_i \in \mathbb{R}^n$  and  $d(x, x') = \min(\|x - x'\|, \|x + x'\|)$ . The mapping  $M(x) = \{|\langle x, f_i \rangle|\}_{i \leq m}$  satisfies*

$$\forall x, x' \in \mathbb{R}^n, \quad A d(x, x') \leq \|M(x) - M(x')\| \leq B d(x, x'), \quad (4)$$

where

$$A = \min_{S \subset \{1 \dots m\}} \sqrt{\lambda_-^2(\mathcal{F}_S) + \lambda_-^2(\mathcal{F}_{S^c})}, \quad (5)$$

$$B = \lambda_+(\mathcal{F}). \quad (6)$$

In particular,  $M$  is injective if and only if for any subset  $S \subseteq \{1, \dots, m\}$ , either  $\mathcal{F}_S$  or  $\mathcal{F}_{S^c}$  is an invertible frame.

A frame  $\mathcal{F}$  satisfying the previous condition is said to be *phase retrievable*.

We now turn our attention to the half-rectification operator, defined as

$$M_\alpha(x) = \rho_\alpha(\mathcal{F}^T x). \quad (7)$$

For that purpose, let us introduce some extra notation. Given a frame  $\mathcal{F} = \{f_1, \dots, f_m\}$ , a subset  $S \subset \{1 \dots m\}$  is *admissible* if

$$\bigcap_{i \in S} \{x; \langle x, f_i \rangle > \alpha_i\} \cap \bigcap_{i \notin S} \{x; \langle x, f_i \rangle < \alpha_i\} \neq \emptyset. \quad (8)$$

We denote by  $\Omega$  the collection of all admissible sets, by  $V_S$  the vector space generated by  $S$ . The following proposition, proved in Section 4, gives a necessary and sufficient condition for the injectivity of the half-rectification.

**Proposition 2.2** *Let  $A_0 = \min_{S \in \Omega} \lambda_-(\mathcal{F}_S|_{V_S})$ . Then the half-rectification operator  $M_\alpha(x) = \rho_\alpha(\mathcal{F}^T x)$  is injective if and only if  $A_0 > 0$ . Moreover, it satisfies*

$$\forall x, x', \quad A_0 \|x - x'\| \leq \|M_\alpha(x) - M_\alpha(x')\| \leq B_0 \|x - x'\|, \quad (9)$$

with  $B_0 = \max_{S \in \Omega} \lambda_+(\mathcal{F}_S) \leq \lambda_+(\mathcal{F})$ .

The half-rectification has the ability to recover the input signal, without the global sign ambiguity. The ability to reconstruct from  $M_\alpha$  is thus controlled by the rank of any matrix  $\mathcal{F}_S$  whose columns are taken from a subset belonging to  $\Omega$ . In particular, since  $S \in \Omega \Rightarrow S^c \in \Omega$ , it results that  $m \geq 2n$  is necessary in order to have  $A_0 > 0$ .

The rectified linear operator creates a partition of the input space into polytopes, defined by (8), and computes a linear operator on each of these regions. A given input  $x$  activates a set  $S_x \in \Omega$ , encoded by the sign of the linear measurements  $\langle x, f_i \rangle - \alpha_i$ . It can be shown that  $|\Omega| = O(m^n)$ , which is much smaller than the total number of subsets  $2^m$  in (5).

As opposed to the absolute value operator, the inverse of  $M_\alpha$ , whenever it exists, can be computed directly by locally inverting a linear operator. Indeed, the coordinates of  $M_\alpha(x)$  satisfying  $M_\alpha(x)_j > \alpha_j$  form a set  $S_x$ , which define a linear model  $\mathcal{F}_{S_x}$  which is invertible by definition. However, this property is not useful as soon as the rectification is cascaded, since one is no longer able to identify the linear model to be inverted by directly inspecting the coordinates.

In order to compare the stability of the half-rectification versus the full rectification, one can modify  $M_\alpha$  so that it maps  $x$  and  $-x$  to the same point. If one considers

$$\widetilde{M}_\alpha(x) = \begin{cases} M_\alpha(x) & \text{if } \lambda_-(\mathcal{F}_{S_x}) > \lambda_-(\mathcal{F}_{S_x^c}) , \\ M_{-\alpha}(-x) & \text{otherwise} . \end{cases}$$

then  $\widetilde{M}_\alpha$  satisfies the following:

**Corollary 2.3**

$$\forall x, x' \in \mathbb{R}^n , \quad \widetilde{A} d(x, x') \leq \|\widetilde{M}_\alpha(x) - \widetilde{M}_\alpha(x')\| \leq \widetilde{B} d(x, x') , \quad (10)$$

with

$$\widetilde{A} = \min_{S \subset \Omega} \max(\lambda_-^2(\mathcal{F}_S), \lambda_-^2(\mathcal{F}_{\overline{S}})) , \quad (11)$$

$$\widetilde{B} = \max_{S \subset \Omega} \lambda_+(\mathcal{F}_S) \leq \lambda_+(\mathcal{F}) , \quad (12)$$

and  $d(x, x') = \min(x - x', x + x')$ , so  $\widetilde{A} \geq 2^{-1/2} A$  and  $\widetilde{B} \leq B$ . In particular, if  $M$  is invertible, so is  $\widetilde{M}_\alpha$ .

It results that the bi-Lipschitz bounds of the half-rectification operator, when considered in under the equivalence  $x \sim -x$ , are controlled by the bounds of the absolute value operator, up to a factor  $2^{-1/2}$ . However, the lower Lipschitz bound (11) consists in a minimum taken over a much smaller family of elements than in (5).

## 2.2 $\ell_p$ Pooling

We give bi-Lipschitz constants of the  $\ell_p$  Pooling and  $\ell_p$  rectified Pooling operators for  $p = 1, 2, \infty$ . From now on, it is assumed that the vectors within each block  $\mathcal{F}_k = \mathcal{F}_{I_k}$  are orthogonal.

From its definition, it follows that pooling operators  $P_p$  and  $R_p$  can be expressed respectively as  $P_p(x) = U_p \circ M$  and  $R_p(x) = \tilde{U}_p \circ M_\alpha$ , which obviously implies that for the pooling to be invertible, it is necessary that the absolute value and rectified operators are invertible too. Naturally, the converse is not true.

The invertibility conditions of the  $\ell_2$  pooling representation have been recently studied in [3], where the authors obtain necessary and sufficient conditions on the frame  $\mathcal{F}$ . We shall now generalize those results, and study how the conditions on the frame  $\mathcal{F}$  should be strengthened in order to guarantee not only phaseless reconstruction, but also reconstruction from pooled measurements for several values of  $p$ .

For that purpose, let us introduce some extra notation. For each  $p = \{1, 2, \infty\}$ , we define a family of perturbations of the frame  $\mathcal{F}$ . We recall that  $\mathcal{F}$  is organized into frames  $\mathcal{F}_k$ ,  $k = 1 \dots K$  whose columns are orthogonal, corresponding to the different pools. For sake of simplicity, and without loss of generality, we assume all the pools have the same size  $|I_k| = d$ .

For  $p = 1$ , we consider

$$\mathcal{Q}_1 = \{(U_k \mathcal{F}_k)_{k \leq K} ; \forall k \leq K, U_k \in \mathbb{R}^{d \times d} U_k^T \mathbf{1} = \mathbf{1} ; \text{rk}(U_k) = d\} , \quad (13)$$

where  $\mathbf{1} = (1, \dots, 1)$ . The family  $\mathcal{Q}_1$  thus contains all the possible changes of basis of the pools  $\mathcal{F}_k$  preserving the average. For  $p = 2$ , we consider

$$\mathcal{Q}_2 = \{(U_k \mathcal{F}_k)_{k \leq K} ; \forall k \leq K, U_k \in \mathbb{R}^{d \times d}, U_k^T U_k = \mathbf{Id}\} . \quad (14)$$

In that case,  $\mathcal{Q}_2$  contains all the orthogonal bases of each subspace  $\mathcal{F}_k$ .

Finally, for  $p = \infty$ , we say that a set of indices  $\gamma = (i_1, i_2, \dots, i_K)$ ,  $i_k \in \{1, \dots, d\}$  is *valid* if

$$\bigcap_{k=1}^K \{x ; s.t. |\langle x, f_{k,i_k} \rangle| > |\langle x, f_{k,j} \rangle| \forall j \neq i_k\} \neq \emptyset ,$$

and denote  $\Gamma$  to be set of all valid  $\gamma$ .  $\Gamma$  thus contains all the possible configurations of locations where the maximum value within each pool is attained. Since  $\mathcal{F}$  is a redundant frame, in general not all configurations will be valid. We then define  $\mathcal{Q}_\infty$  as the collection

$$\begin{aligned} \mathcal{Q}_\infty = & \{(f'_{k,j})_{k \leq K, j \leq d} ; \exists \gamma_1, \gamma_2 \in \Gamma \text{ s.t. } \forall k, \text{span}(f'_{k,j})_{j \leq d} = \mathcal{F}_k ; \\ & (f'_{k,\gamma_1(k)} f'_{k,\gamma_2(k)}) = U_t(f'_{k,\gamma_1(k)} f'_{k,\gamma_2(k)})\} , \end{aligned} \quad (15)$$

where  $U_t$  is a  $2 \times 2$  matrix of the form

$$\begin{pmatrix} t_1 + t_2 & t_1 - t_2 \\ 2 - t_1 - t_2 & t_2 - t_1 \end{pmatrix} .$$

For each  $p$ , the families  $\mathcal{Q}_p$  thus contain all possible bases of the subspaces  $\mathcal{F}_k$  which satisfy a specific set of constraints, which depend upon the geometry of the  $\ell_p$  balls.

The following theorem, proved in section 4, computes upper and lower bounds of the Lipschitz constants of  $P_p$ .

**Theorem 2.4** *Let  $p = \{1, 2, \infty\}$ . The  $\ell_p$  pooling operator  $P_p$  satisfies*

$$\forall x, x'; \quad A_p d(x, x') \leq \|P_p(x) - P_p(x')\| \leq B_p d(x, x') , \quad (16)$$

where

$$\begin{aligned} A_p &= \min_{\mathcal{F}' \in \mathcal{Q}_p} \min_{S \subset \{1 \dots m\}} \sqrt{\lambda_-^2(\mathcal{F}'_S) + \lambda_-^2(\mathcal{F}'_{S^c})} , \\ B_p &= \alpha_p \lambda_+(\mathcal{F}) \end{aligned} \quad (17)$$

with  $\alpha_1 = \sqrt{d}$ ,  $\alpha_2 = 1$  and  $\alpha_\infty = d$ .

Finally, we also consider the rectified  $\ell_p$  pooling case. For simplicity, we shall concentrate in the case where the pools have dimension  $d = 2$ . For that purpose, for each  $p = \{1, 2, \infty\}$ , and each  $x, x'$ , we consider a modification of the families  $\mathcal{Q}_p$ , by replacing each sub-frame  $\mathcal{F}_k$  by  $\mathcal{F}_{I_k \cap S_x \cap S_{x'}}$ , that we denote  $\tilde{\mathcal{Q}}_{p,x,x'}$ .

**Corollary 2.5** *Let  $d = 2$ . Then the rectified  $\ell_p$  pooling operator  $R_p$  satisfies*

$$\forall x, x'; \quad \tilde{A}_p d(x, x') \leq \|R_p(x) - R_p(x')\| \leq B_p d(x, x') , \quad (18)$$

where

$$\begin{aligned} \tilde{A}_p &= \inf_{x, x'} \min_{\mathcal{F}' \in \tilde{\mathcal{Q}}_{p,x,x'}} \min_{S \subset S_x \cap S_{x'}} \left( \lambda_-^2(\mathcal{F}_{S_x \cup S_{x'} \setminus (S_x \cap S_{x'})}) + \right. \\ &\quad \left. \lambda_-^2(\mathcal{F}'_S) + \lambda_-^2(\mathcal{F}'_{S^c}) \right)^{1/2} , \end{aligned}$$

with  $\alpha_1 = \sqrt{d}$ ,  $\alpha_2 = 1$  and  $\alpha_\infty = d$ .

Theorem 2.4 and Corollary 2.5 thus give a lower Lipschitz bound which gives sufficient guarantees for the inversion of pooling representations. In all configurations, we ask that a certain perturbation of the analysis frame  $\mathcal{F}$  results in a phase retrievable frame. The perturbations depend upon the geometries of the different  $\ell_p$  balls, but in all cases they correspond to specific class of bases for each subspace  $\mathcal{F}_k$ . Our lower Lipschitz bounds seem to indicate that  $\ell_2$  pooling requires a weaker condition over  $\ell_\infty$  and  $\ell_1$ . However, the bounds for  $p = 1, \infty$  are not known to be tight, as opposed to the  $\ell_2$  case, where one can easily show that  $A_2$  is tight. Corollary 2.5 indicates that, in the case  $d = 2$ , the lower Lipschitz bounds are sharper than the non-rectified case, in consistency with the results of section 2.1. The general case for  $d > 2$  remains an open issue.

### 3 Numerical Experiments

#### 3.1 Algorithms

##### 3.1.1 Alternating minimization

A greedy method for recovering the phase from the modulus of complex measurements is given in [5]; this method naturally extends to the case at hand. As above, denote the frame  $\{f_1, \dots, f_m\} = \mathcal{F}$ , let  $\mathcal{F}_k$  be the frame vectors in the  $k$ th block, and set  $I_k$  to be the indices of the  $k$ th block. Let  $\mathcal{F}^{(-1)}$  be the pseudoinverse of  $\mathcal{F}$ ; set  $(P_p(x))_k = \|\mathcal{F}_k x\|_p$ . Starting with an initial signal  $x^0$ , update

1.  $y_{I_k}^{(n)} = (P_p(x))_k \frac{\mathcal{F}_k x^{(n)}}{\|\mathcal{F}_k x^{(n)}\|_p}$ ,  $k = 1 \dots K$ ,
2.  $x^{(n+1)} = \mathcal{F}^{(-1)} y^{(n)}$ .

This approach is not, as far as we know, guarantee to converge to the correct solution, even when  $P_p$  is invertible. However, in practice, if the inversion is easy enough, or if  $x_0$  is close to the true solution, the method can work well. Moreover, this algorithm can be run essentially unchanged for each  $\ell_p$ ; for half rectification, we only use the nonnegative entries in  $y$  for reconstruction.

In the experiments below, we will use random, Gaussian i.i.d.  $\mathcal{F}$ , but also we will use the outputs of dictionary learning with block sparsity. The  $\mathcal{F}$  generated this way is not really a frame, as the condition number of a trained dictionary on real data is often very high. In this case, we will renormalize each data point to have norm 1, and modify the update  $x^{(n+1)} = \mathcal{F}^{(-1)} y^{(n)}$  to

2.  $x^{(n+1)} = \arg \min_{\|x\|_2=1} \|\mathcal{F}x - y^{(n)}\|^2$ .

In practice, this modification might not always be possible, since the norm  $\|x\|$  is not explicitly presented in  $P_p$ . However, in the classical setting of Fourier measurements and positive  $x$ , this information is available. Moreover, our empirical experience has been that using this regularization on well conditioned analysis dictionaries offers no benefit; in particular, it gives no benefit with random analysis matrices.

##### 3.1.2 Phaselift and Phasecut

Two recent algorithms [4] and [11] are guaranteed with high probability to solve the (classical) problem of recovering the phase of a complex signal from its modulus, given enough random measurements. In practice both perform better than the greedy alternating minimization. However, it is not obvious to us how to adapt these algorithms to the  $\ell_p$  setting.



### 3.1.3 Nearest neighbors regression

We would like to use the same basic algorithm for all settings to get an idea of the relative difficulty of the recovery problem for different  $p$ , but also would like an algorithm good recovery performance. If our algorithm simply returns poor results in each case, differences between the case might be masked.

The alternating minimization can be very effective when well initialized. When given a training set of the data to recover, we use a simple regression to find  $x_0$ . Fix a number of neighbors  $q$  (in the experiments below we use  $q = 10$ , and suppose  $X$  is the training set). Set  $G = P_p(X)$ , and for a new point  $x$  to recover from  $P_p(x)$ , find the  $q$  nearest neighbors in  $G$  of  $P_p(x)$ , and take their principal component to serve as  $x_0$  in the alternating minimization algorithm. We use the fast neighbor searcher from [10] to accelerate the search.

## 3.2 Experiments

We discuss results on the MNIST dataset, available at <http://yann.lecun.com/exdb/mnist/>, and on  $16 \times 16$  patches drawn from the VOC dataset, available at <http://pascallin.ecs.soton.ac.uk/challenges/VOC/voc2012/>. For each of these data sets, we run experiments with random dictionaries and adapted dictionaries. The basic setup of the experiments in each case is the same: we vary the number of measurements (that is, number of pools) over some range, and attempt to recover the original signal from the  $\ell_p$  pooled measurements. We record the average angle between the recovered signal  $r$  and the original  $x$ , that is, we use  $|r^T x|^2 / (||r||^2 ||x||^2)$  as the measure of success in recovery. In each case the random analysis dictionary  $\mathcal{F}$  is built by fixing a size parameter  $m$ , and generating a Gaussian i.i.d. matrix  $\mathcal{F}_0$  of size  $2m \times n$ , where  $n = 100$  for MNIST, and  $n = 256$  for VOC. Each pair of rows of  $\mathcal{F}_0$  is then orthogonalized to obtain  $\mathcal{F}$ ; that is we use groups of size 2, where the pair of elements in each group are orthogonal. This allows us to use standard phase recovery software in the  $\ell_2$  case to get a baseline. We used the ADMM version of phaselift from [8] and the phasecut algorithm of [11]. For all of our data sets, the latter gave better results (note that phasecut can explicitly use the fact that the solution to the problem is real, whereas that version of phaselift cannot), so we report only the phasecut results. In the experiments with adapted dictionaries, the dictionary is built using block OMP and batch updates with a K-SVD type update; in this case,  $\mathcal{F}$  is the transpose of the learned dictionary. We again use groups of size 2 in the adapted dictionary experiments. We also run experiments where the data and the dictionary are both Gaussian i.i.d.; in this case, we do not use the nearest neighbor regressor or adapted dictionaries.

### 3.2.1 Random data and measurements

We run two sets of experiments, with  $n = 20$  and  $n = 40$ . The data is generated Gaussian normal, i.i.d. as is the analysis frame; although as in all the experiments, each pair of

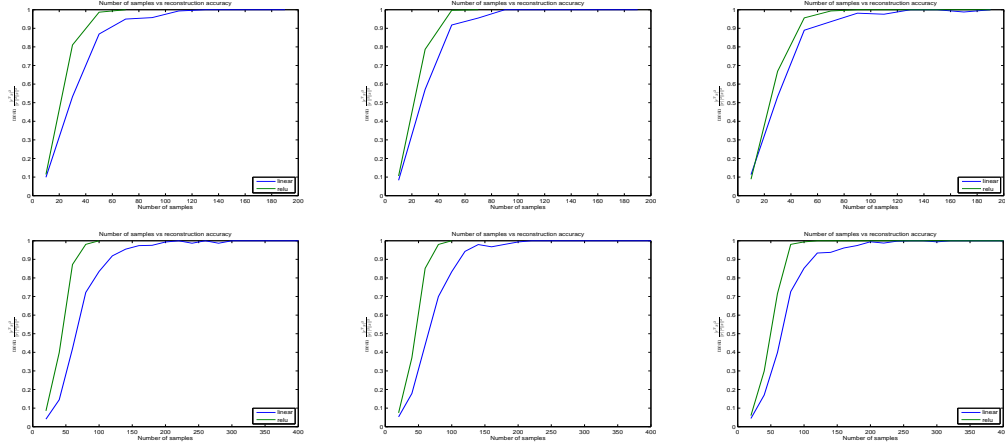


Figure 1: Average recovery angle using alternating projections. The vertical axis measures the average value of  $|r^T x|^2 / (\|r\|^2 \|x\|^2)$  over 50 random test points. The horizontal axis is the number of measurements (the size  $m$  of the analysis dictionary is twice the  $x$  axis in this experiment). The leftmost figure is  $\ell_1$  pooling, the middle  $\ell_2$ , and the right max pooling. In the top row each  $x$  is Gaussian i.i.d. in  $\mathbb{R}^{20}$ , in the bottom row, in  $\mathbb{R}^{40}$ .

rows of the analysis frame are orthogonalized. We consider  $m$  in the range from  $n/2$  to  $8n$ . On this data set, phaselift outperforms alternating minimization; see the supplementary material.

### 3.2.2 MNIST

The MNIST data set consists of 70000  $28 \times 28$  images of handwritten digits. The data set is organized into a standard training set of 60000 points and test set of 10000 points. The points are projected to  $\mathbb{R}^{100}$  via PCA. In this experiment, we let the number of dictionary elements range from 60 to 600 (that is, 30 to 300 measurements). On this data set, alternating minimization with nearest neighbor initialization gives exact reconstruction by 130 measurements; for comparison, Phaselift at  $m = 130$  has mean square angle of .48; see the supplementary material.

### 3.2.3 image patches

We draw approximately 5 million  $16 \times 16$  grayscale image patches from the PASCAL VOC data set; these are sorted by variance, and the largest variance 1 million are kept. The mean is removed from each patch. These are split into a training set of 900000 patches and a test set of 100000 patches. In this experiment, we let  $m$  range from 30 to 830. On

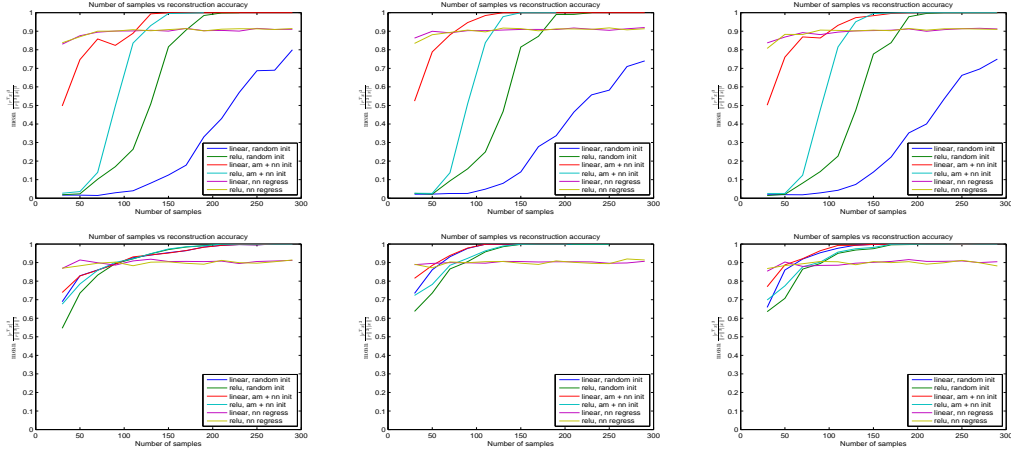


Figure 2: Average recovery angle using alternating projections on MNIST data points. The vertical axis measures the average value of  $|r^T x|^2 / (\|r\|^2 \|x\|^2)$  over 50 random test points. The horizontal axis is the number of measurements (the size of the analysis dictionary is twice the  $x$  axis in this experiment). The leftmost figure is  $\ell_1$  pooling, the middle  $\ell_2$ , and the right max pooling. In the top row the analysis dictionary is Gaussian i.i.d.; in the bottom row, generated by block OMP/KSVD with 5 nonzero blocks of size 2.

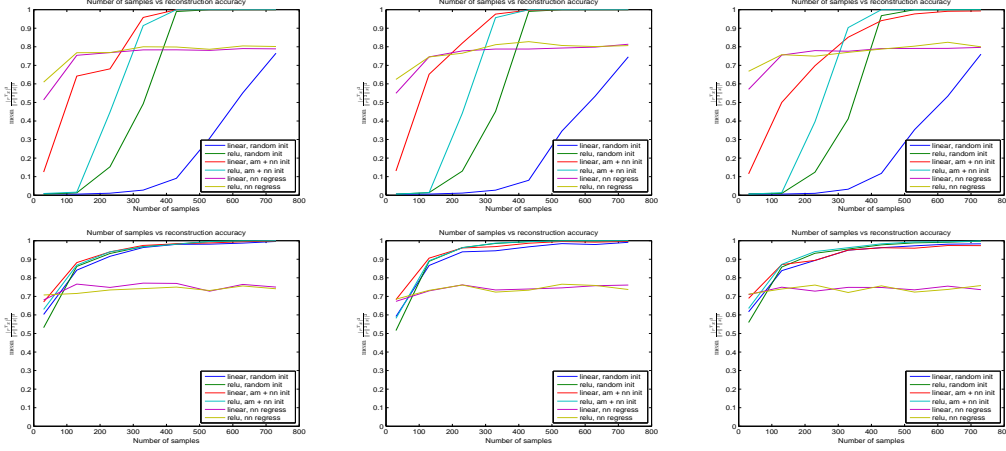


Figure 3: Average recovery angle using alternating projections on image patch data points. The vertical axis measures the average value of  $|r^T x|^2 / (||r||^2 ||x||^2)$  over 50 random test points. The horizontal axis is the number of measurements (the size of the analysis dictionary is twice the  $x$  axis in this experiment). The leftmost figure is  $\ell_1$  pooling, the middle  $\ell_2$ , and the right max pooling. In the top row the analysis dictionary is Gaussian i.i.d.; in the bottom row, generated by block OMP/KSVD with 5 nonzero blocks of size 2.

this data set, by  $m = 330$  measurements, alternating minimization with nearest neighbor initialization recovers mean angle of .97; for comparison, Phaselift at  $m = 330$  has mean angle of .39; see the supplementary material.

### 3.3 Analysis

The experiments show that:

- For every data set, with random initializations and dictionaries, recovery is easier with half rectification before pooling than without.
- $\ell_\infty$ ,  $\ell_1$ , and  $\ell_2$  pooling are all roughly the same difficulty to invert.
- Good initialization improves performance; indeed, alternating minimization with nearest neighbor regression outperforms phaselift and phasecut (which of course do not have the luxury of samples from the prior, as the regressor does).
- Adapted analysis “frames” (with regularization) are easier to invert than random analysis frames, with or without regularization.

Each of these conclusions is unfortunately only true up to the optimization method- it may be true that a different optimizer will lead to different results. With learned initializations

and alternating minimization, recovery results can be better without half rectification. Note this is only up until the point where the alternating minimization gets better than the learned initialization without any refinement, and is especially true for random dictionaries. The simple interpretation is that the reconstruction step 2 of the alternating minimization just does not have a large enough span with roughly half the entries removed; that is, this is an effect of the optimization, not of the difference between the difficulty of the problem itself.

## 4 Proofs of results in Section 2

### 4.1 Proof of Proposition 2.2

Let us first show that  $A_0 > 0$  is sufficient to construct an inverse of  $M_\alpha$ . Let  $x \in \mathbb{R}^n$ . By definition, the coordinates of  $M_\alpha(x) > \alpha$  correspond to

$$S_x = \{i \text{ s.t. } \langle x, f_i \rangle > \alpha_i\} \subset \{1, \dots, m\} ,$$

which in particular implies that  $x$  is known to lie in  $V_{S_x}$ , the subspace generated by  $S_x$ . But the restriction  $\mathcal{F}_{S_x}$  is a linear operator, which can be inverted in  $V_S$  as long as  $\lambda_-(\mathcal{F}_{S_x}|_{V_S}) \geq A_0 > 0$ .

Let us now show that  $A_0 > 0$  is also necessary. Let us suppose that for some  $S$ ,  $\mathcal{F}_S$  is such that  $\lambda_-(\mathcal{F}_S|_{V_S}) = 0$ . It results that there exists  $\eta \in V_S$  such that  $\|\eta\| > 0$  but  $\|\mathcal{F}_S \eta\| = 0$ . Since  $S$  is a cone, we can find  $x \in S$  and  $\epsilon \neq 0$  small enough such that  $x + \epsilon \eta \in S$ . It results that  $M_\alpha(x) = M_\alpha(x + \epsilon \eta)$  which implies that  $M_\alpha$  cannot be injective.

Finally, let us prove (9). If  $x, x'$  are such that  $S = S_x = S_{x'}$ , then

$$\|M_\alpha(x) - M_\alpha(x')\| = \|\mathcal{F}_S(x - x')\| \geq A_0 \|x - x'\| .$$

If  $S_x \neq S_{x'}$ , we have that  $|M_\alpha(x)_i - M_\alpha(x')_i| = |\langle x - x', f_i \rangle|$  if  $i \in S_x \cap S_{x'}$  and  $|M_\alpha(x)_i - M_\alpha(x')_i| \geq |\langle x - x', f_i \rangle|$  if  $i \in S_x \cup S_{x'}$ ,  $i \notin S_x \cap S_{x'}$ . It results that

$$\|M_\alpha(x) - M_\alpha(x')\| \geq \|\mathcal{F}_{S_x \cup S_{x'}}(x - x')\| \geq A_0 \|x - x'\| .$$

□.

### 4.2 Proof of Theorem 2.4

The upper Lipschitz bound is obtained by observing that, in dimension  $d$ ,

$$\forall y \in \mathbb{R}^d , \quad \|y\|_1 \leq \sqrt{d} \|y\|_2 , \quad \|y\|_\infty \leq \|y\|_2 .$$

It results that

$$\begin{aligned} \|P_p(x) - P_p(x')\| &\leq \alpha_p \|P_2(x) - P_2(x')\| \\ &= \alpha_p \|M(x) - M(x')\| \leq \alpha_p \lambda_+(\mathcal{F}) . \end{aligned} \tag{19}$$

Let us now concentrate on the lower Lipschitz bound. For  $p = 2$ , given  $x, x' \in \mathbb{R}^n$ , we first consider a rotation  $\tilde{\mathcal{F}}_k$  on each subspace  $\mathcal{F}_k$  such that  $\langle x, \tilde{f}_{k,j} \rangle = \langle x', \tilde{f}_{k,j} \rangle = 0$  for  $j > 2$ , which always exists. If now we modify  $\tilde{\mathcal{F}}_k$  by applying a rotation of the remaining two-dimensional subspace such that  $x$  and  $x'$  are bisected, one can verify that

$$\begin{aligned} (\|\mathcal{F}_k x\|_2 - \|\mathcal{F}_k x'\|_2)^2 &= (\|\tilde{\mathcal{F}}_k x\|_2 - \|\tilde{\mathcal{F}}_k x'\|_2)^2 \\ &= (|\langle x, \tilde{f}_{k,1} \rangle| - |\langle x', \tilde{f}_{k,1} \rangle|)^2 \\ &\quad + (|\langle x, \tilde{f}_{k,2} \rangle| - |\langle x', \tilde{f}_{k,2} \rangle|)^2, \end{aligned}$$

which implies, by denoting  $M(x) = (|\langle x, \tilde{f}_{k,j} \rangle|)_{k,j}$ , that  $\|P_2(x) - P_2(x')\| = \|M(x) - M(x')\|$ . Since  $\tilde{\mathcal{F}} \in \mathcal{Q}_2$ , it results from Proposition 2.1 that

$$\begin{aligned} \|P_2(x) - P_2(x')\| &\geq d(x, x') \min_{S \subset \{1 \dots m\}} \sqrt{\lambda_-^2(\tilde{\mathcal{F}}_S) + \lambda_-^2(\tilde{\mathcal{F}}_{S^c})} \\ &\geq d(x, x') A_2. \end{aligned} \tag{20}$$

For  $p = 1$  and  $p = \infty$  we use a similar argument. Given  $x, x' \in \mathbb{R}^n$ , we will construct a frame  $\tilde{\mathcal{F}} = (\tilde{\mathcal{F}}_k)_{k \leq K} \in \mathcal{Q}_p$  such that

$$\forall k, x, \|\tilde{\mathcal{F}}_k x\|_p = \|\mathcal{F}_k x\|_p, \tag{21}$$

and such that

$$\forall k, \forall j = 2, \dots, d, |\langle x, \tilde{f}_{k,j} \rangle| = |\langle x', \tilde{f}_{k,j} \rangle|, \tag{22}$$

and when  $p = \infty$  also satisfies

$$\max_{j=1,2} (|\langle x, \tilde{f}_{k,j} \rangle|) \geq \max_{j' > 2} |\langle x, \tilde{f}_{k,j'} \rangle|. \tag{23}$$

Let us first show how (21, 22) imply (16). For  $p = 1$ , we have that

$$\begin{aligned} (\|\mathcal{F}_k x\|_1 - \|\mathcal{F}_k x'\|_1)^2 &= (\|\tilde{\mathcal{F}}_k x\|_1 - \|\tilde{\mathcal{F}}_k x'\|_1)^2 \\ &= (|\langle x, \tilde{f}_{k,1} \rangle| - |\langle x', \tilde{f}_{k,1} \rangle|)^2 \\ &= \sum_{j=1}^d (|\langle x, \tilde{f}_{k,j} \rangle| - |\langle x', \tilde{f}_{k,j} \rangle|)^2, \end{aligned}$$

which implies, by denoting  $M(x) = (|\langle x, \tilde{f}_{k,j} \rangle|)_{k,j}$ , that  $\|P_1(x) - P_1(x')\| = \|M(x) - M(x')\|$ , and hence

$$\|P_1(x) - P_1(x')\| \geq d(x, x') A_1. \tag{24}$$

For  $p = \infty$ , thanks to (23) it results that  $P_\infty(x)$ ,  $P_\infty(x')$  only depend upon the first two coordinates. Since in two dimensions the  $\ell_1$  ball and the  $\ell_\infty$  ball are equivalent under a  $\pi/4$  rotation, it results from (24) that

$$\|P_\infty(x) - P_\infty(x')\| \geq d(x, x')A_\infty . \quad (25)$$

Let us finally show how to obtain the frames satisfying (21), (22) and (23). Let  $p = 1$  and fix a subspace  $\mathcal{F}_k$ . We proceed by applying successive transformations of the form

$$\begin{aligned} \tilde{f}_{k,j} &= (1 - \alpha_j)f_{k,j} + \alpha_{j+1}f_{k,j+1} \\ \tilde{f}_{k,j+1} &= \alpha_j f_{k,j} + (1 - \alpha_{j+1})f_{k,j+1} . \end{aligned} \quad (26)$$

One can verify that this transformation preserves the  $\ell_1$  norm as long as the signs of  $\langle x, \tilde{f}_{k,j} \rangle$ ,  $\langle x, \tilde{f}_{k,j+1} \rangle$  are the same as those of  $\langle x, f_{k,j} \rangle$ ,  $\langle x, f_{k,j+1} \rangle$ . We visit the coordinates  $j = 1 \dots d$  in increasing order. The signs of  $\langle x, f_{k,j} \rangle$ ,  $\langle x', f_{k,j} \rangle$ ,  $\langle x, f_{k,j+1} \rangle$  and  $\langle x', f_{k,j+1} \rangle$  determine a quadrant for  $x$  and  $x'$  respectively. If  $|\langle x, f_{k,j} \rangle| = |\langle x', f_{k,j} \rangle|$ , we skip the coordinate. Otherwise, suppose without loss of generality that  $|\langle x, f_{k,j} \rangle| > |\langle x', f_{k,j} \rangle|$ . Depending on the sign of these scalar products, in order to achieve  $|\langle x, \tilde{f}_{k,j} \rangle| = |\langle x', \tilde{f}_{k,j} \rangle|$ , we either need to increase  $\langle x, f_{k,j} \rangle$  and decrease  $\langle x', f_{k,j} \rangle$  or viceversa. But observe that can always achieve this using (26) by adjusting  $\alpha_j$  and  $\alpha_{j+1}$ . Since each transformation of the form (26) can be written as  $\tilde{\mathcal{F}}_k = U\mathcal{F}_k$  with  $U\mathbf{1} = \mathbf{1}$ , it results that any product  $U = U_1, U_2, \dots, U_d$  also satisfies  $U\mathbf{1} = \mathbf{1}$ , and hence that such composition belongs to  $\mathcal{Q}_1$ .

Similarly, for  $p = \infty$  we use the same strategy. Given  $x, x'$ , for each  $k$  there are at least  $d - 2$  coordinates which do not influence the value of  $P_\infty(x)$  nor  $P_\infty(x')$ . We can thus find a change of basis on this  $d - 2$  subspace such that  $|\langle x, \tilde{f}_{k,j} \rangle| = |\langle x', \tilde{f}_{k,j} \rangle|$  for  $j > 2$ . In the remaining 2 dimensions, by applying the transformation

$$\tilde{f}_{k,1} = \frac{1}{2}(f_{k,1} + f_{k,2}) , \quad \tilde{f}_{k,2} = \frac{1}{2}(f_{k,1} - f_{k,2}) , \quad (27)$$

we verify that

$$\max(|\langle x, f_{k,1} \rangle|, |\langle x, f_{k,2} \rangle|) = |\langle x, \tilde{f}_{k,1} \rangle| + |\langle x, \tilde{f}_{k,2} \rangle| ,$$

and hence, by using a final transformation of the form (26) in this two-dimensional subspace, we obtain (21) and (22). Since by definition the family  $\mathcal{Q}_\infty$  contains arbitrary bases on  $d - 2$  subspaces of each  $\mathcal{F}_k$  and a final transformation which is the product of (27) and (26), the proof of (17) is completed.  $\square$ .

### 4.3 Proof of Corollary 2.5

Given  $x, x'$ , let  $I$  denote the groups  $I_k$ ,  $k \leq K$  such that  $S_x \cap S_{x'} \cap I_k = I_k$ . It results that

$$\begin{aligned} \|R_p(x) - R_p(x')\|^2 &= \sum_{k \in I} |R_p(x)_k - R_p(x')_k|^2 + \sum_{k \notin I} |R_p(x)_k - R_p(x')_k|^2 \\ &\geq \sum_{k \in I} |R_p(x)_k - R_p(x')_k|^2 + \sum_{k \notin I} (\|M_0(x)|_{I_k} - M_0(x')|_{I_k}\|)^2 . \end{aligned}$$

On the groups in  $I$  we can apply the same arguments as in theorem 2.4, and hence find a frame  $\tilde{\mathcal{F}}$  from the family  $\tilde{\mathcal{Q}}_{p,x,x'}$  such that

$$\|R_p(x) - R_p(x')\|_I = \|M(x) - M(x')\| ,$$

with  $M(x) = (|\langle x, \tilde{f}_{k,j} \rangle|)_{k \in I, j}$  and  $\{\tilde{f}_{k,j}\} \in \tilde{\mathcal{Q}}_{p,x,x'}$ . Then, by following the same arguments used previously, it results from the definition of  $\tilde{A}_p$  that

$$\|R_p(x) - R_p(x')\| \geq \tilde{A}_p d(x, x') .$$

Finally, the upper Lipschitz bound is obtained by noting that

$$\|M_\alpha(x) - M_\alpha(x')\| \leq \|\mathcal{F}(x - x')\| ,$$

and using the same argument as in (19)  $\square$ .

## 5 Conclusion

We have studied conditions under which neural network layers of the form (1) and (2) preserve signal information. As one could expect, recovery from pooling measurements is only guaranteed under large enough redundancy and configurations of the subspaces, which depend upon which  $\ell_p$  is considered.

There is much to be done to fully understand the invertibility of these layers. Our results just barely touch on the distribution of the data; but the experiments make it clear (see also [8]) that knowing more information about the data changes the invertibility of the mappings. From an algorithmic perspective, there has been much work in inverting  $\ell_2$  pooling with no nonlinearity. What are correct algorithms for  $\ell_p$  inversion, perhaps with half rectification?

## References

- [1] Radu Balan, Pete Casazza, and Dan Edidin. On signal reconstruction without phase. *Applied and Computational Harmonic Analysis*, 20(3):345–356, May 2006.
- [2] Radu Balan and Yang Wang. Invertibility and robustness of phaseless reconstruction, 2013.
- [3] Jameson Cahill, Peter G. Casazza, Jesse Peterson, and Lindsey Woodland. Phase retrieval by projections, 2013.
- [4] Emmanuel J. Candes, Thomas Strohmer, and Vladislav Voroninski. Phaselift: Exact and stable signal recovery from magnitude measurements via convex programming. *Communications on Pure and Applied Mathematics*, 66(8):1241–1274, 2013.



- [5] R. W. Gerchberg and W. Owen Saxton. A practical algorithm for the determination of the phase from image and diffraction plane pictures. *Optik*, 35:237–246, 1972.
- [6] A. Hyvärinen and P. Hoyer. A two-layer sparse coding model learns simple and complex cell receptive fields and topography from natural images. *Vision Research*, 41(18):2413–2423, August 2001.
- [7] Koray Kavukcuoglu, Marc’Aurelio Ranzato, Rob Fergus, and Yann LeCun. Learning invariant features through topographic filter maps. In *Proc. International Conference on Computer Vision and Pattern Recognition (CVPR’09)*. IEEE, 2009.
- [8] Henrik Ohlsson, Allen Y. Yang, Roy Dong, and S. Shankar Sastry. Cprl – an extension of compressive sensing to the phase retrieval problem. In Peter L. Bartlett, Fernando C. N. Pereira, Christopher J. C. Burges, Léon Bottou, and Kilian Q. Weinberger, editors, *NIPS*, pages 1376–1384, 2012.
- [9] Y. Ohlsson, H. Eldar. On conditions for uniqueness for sparse phase retrieval, 2013.
- [10] A. Vedaldi and B. Fulkerson. VLFeat: An open and portable library of computer vision algorithms. <http://www.vlfeat.org/>, 2008.
- [11] Irène Waldspurger, Alexandre d’Aspremont, and Stéphane Mallat. Phase recovery, maxcut and complex semidefinite programming, 2012.